ACADEMIC PRESS

Available online at www.sciencedirect.com

SCIENCE DIRECT®

Journal of Sound and Vibration 267 (2003) 1143–1156

JOURNAL OF SOUND AND VIBRATION

www.elsevier.com/locate/jsvi

Determination of the steady state response of viscoelastically point-supported rectangular specially orthotropic plates by an energy-based finite difference method

T. Kocatürk*, G. Altintaş

Faculty of Civil Engineering, Yildiz Technical University, Yildiz-Besiktas, Istanbul 80750, Turkey

Received 19 March 2002; accepted 31 October 2002

Abstract

A method based on a variational procedure in conjunction with a finite difference method is used to examine the free vibration characteristics and steady state response to a sinusoidally varying force applied at the center of a viscoelastically point-supported orthotropic elastic plate of rectangular shape. Using the energy-based finite difference method, the problem is reduced to the solution of a system of algebraic equations. The influence of the mechanical properties, and of the damping of the supports to the mode shapes and to the steady state response of viscoelastically point-supported rectangular plates is investigated numerically for a concentrated load at the center for various values of the mechanical properties characterizing the anisotropy of the plate material and for various damping ratios. The results are given for the frequencies and mode shapes of the first three symmetrical modes. Convergence studies are made. The validity of the present approach is demonstrated by comparing the results with other solutions based on the Kirchhoff–Love plate theory.

1. Introduction

This problem is of considerable interest to engineers designing panels at isolated points. The free vibration analysis of rectangular isotropic plates supported at various points and based on the Kirchhoff–Love plate theory has been investigated and is well known. However, it appears that there are only a limited number of studies on the steady state response of viscoelastically point-supported plates.

*Corresponding author. Tel.: +90 212-259-70-70/2775; fax: +90 212-236-41-77.
E-mail address: kocaturk@yildiz.edu.tr (T. Kocatürk).

0022-460X/03/$ - see front matter
doi:10.1016/S0022-460X(03)00201-3

A considerable number of publications have been concerned with the free vibration analysis of rectangular isotropic and orthotropic plates supported at various points and based on the Kirchhoff–Love plate theory. A survey of some of these studies was given by Kocatürk [1]. Although there are many studies of the free vibration analysis of rectangular plates supported at various points, there are only a limited number of studies on the steady state response of point-supported rectangular plates. The steady state response to a sinusoidally varying force is determined for a viscoelastically point-supported square or rectangular plate by Yamada et al. [2] by using the generalized Galerkin method. A generalization of this study to orthotropic rectangular plates was investigated by Kocatürk [1]. In the present study, an extension of the problem investigated by Kocatürk [1] is analyzed by using a method based on a variational procedure in conjunction with a finite difference technique for minimizing the peak values of the force transmissibilities. Also, by using the same procedure, parametric instability of rectangular plates by the energy-based finite difference method was investigated by Singh and Dey [3].

In many branches of modern industry, structural elements, such as plates, are fabricated from composite materials. For this reason, the present investigation may be considered to be a problem of the mechanics of elements fabricated from composite materials. The purpose of the present work is to analyze the steady state response of a viscoelastically point-supported orthotropic plate to a sinusoidally varying force for various values of the mechanical properties characterizing the anisotropy of the plate material by using a finite difference energy method. The problems considered are solved within the framework of the Kirchhoff–Love hypothesis. The convergence study is based on the numerical values obtained for various mesh sizes. In the numerical examples, the natural frequency parameters, nodal patterns and steady state responses to a sinusoidally varying force are determined for the first three symmetrical mode types. The accuracy of the results is partially established by comparison with previously published accurate results for the corner point-supported plates based on thin plate theory.

2. Analysis

Consider a viscoelastically point-supported rectangular elastic orthotropic plate of side lengths a, b and thickness h under a concentrated force $F(t)$ at the center of the plate as shown in Fig. 1, where k_i is the spring constant, c_i is the damping coefficient, $P_i(X_{1i}, X_{2i})$ is the support force of a point support at the ith support. The axes of the elastic symmetry of the plate material coincides with the OX_1- and OX_2-axis. Therefore, the plate is specially orthotropic. Also, the co-ordinate axes OX_1 and OX_2 are oriented parallel to the edges of the plate with the origin at O. Because the plate is orthotropic and the supports are viscoelastic, there are many parameters to be considered. Therefore, although it is possible to take lots of point supports at arbitrary points, in the numerical investigations here, for brevity of the study, it will be considered that the plate is supported symmetrically at the four corner points and k_i and c_i are taken to have the same respective values at all the supports denoted by $k_i = k_s$ and $c_i = c_s$. Thus, in the considered loading and support conditions, only symmetrical vibrations arise in the plate. Under the above mentioned conditions, the steady state responses of the viscoelastically corner point-supported plate to a sinusoidally varying force for various damping values will be determined by using a variational method in conjunction with a finite difference technique. The procedure essentially

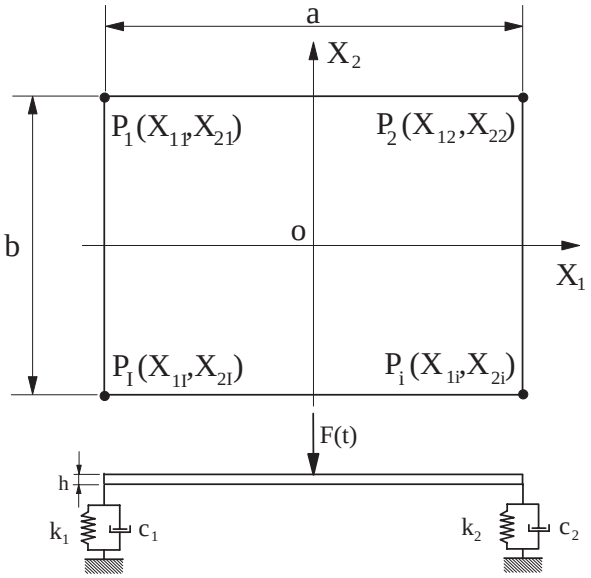

Fig. 1. Viscoelastically point-supported rectangular anisotropic (orthotropic) plate subjected to an external force.

consists of dividing the surface of the plate into a regular gridwork, then by means of difference operators the total energy of flexural vibrations is discretized in terms of gridpoint deflections. Application of Lagrange's equation with respect to each gridpoint deflection in succession yields a set of linear algebraic equations. For a plate undergoing sinusoidally varying force $F(t) = Qe^{i\omega t}$, where ω is radian frequency, the strain energy of bending in Cartesian co-ordinates is given by

$$U = \frac{1}{2}\int_{-a/2}^{a/2}\int_{-b/2}^{b/2}\left[D_{11}\left(\frac{\partial^2 W}{\partial X_1^2}\right)^2 + 2D_{11}v_{21}\frac{\partial^2 W}{\partial X_1^2}\frac{\partial^2 W}{\partial X_2^2} + D_{22}\left(\frac{\partial^2 W}{\partial X_2^2}\right)^2 + 4D_{66}\left(\frac{\partial^2 W}{\partial X_1 \partial X_2}\right)^2\right] \mathrm{d}X_1\,\mathrm{d}X_2. \tag{1}$$

In Eq. (1), D_{11}, D_{22}, D_{66} are expressed as follows:

$$D_{11} = \frac{E_1' h^3}{12}, \quad D_{22} = \frac{E_2' h^3}{12}, \quad D_{66} = \frac{G_{12} h^3}{12}, \tag{2}$$

where G_{12} is shear modulus. E_1', E_2' are derived as follows:

$$\frac{v_{12}}{E_1} = \frac{v_{21}}{E_2}, \quad e = \frac{E_2}{E_1}, \quad E_1' = \frac{E_1}{1 - v_{21}^2/e}, \quad E_2' = \frac{E_1 e}{1 - v_{21}^2/e}, \tag{3}$$

Here E_1, E_2 are Young's moduli in the OX_1 and OX_2 directions, respectively, and v_{21} is the Poisson ratio for the strain response in the X_1 direction due to an applied stress in the X_2 direction. The potential energy of the external force is

$$F_e = -F(t)W. \tag{4}$$

As it can be seen from Eq. (4), to determine the potential energy of the external force, it is necessary to use the displacement of the location of the force. In the present study, the location of the force is chosen as a gridpoint. If the force is not at any gridpoint, for calculating the potential

energy of the external force, the displacement of the location of the external force can be calculated by using an interpolation procedure with respect to the neighbor gridpoints. The kinetic energy of vibration is

$$T = \frac{1}{2}\int_{-a/2}^{a/2}\int_{-b/2}^{b/2} \rho h\left(\frac{\partial W}{\partial t}\right)^2 \mathrm{d}X_1\,\mathrm{d}X_2 \tag{5}$$

and the additive strain energy and dissipation function of viscoelastic supports are

$$F_s = \frac{1}{2}\sum_{i=1}^{4} k_i W_{Si}^2, \quad D = \frac{1}{2}\sum_{i=1}^{4} c_i(\dot{W}_{Si})^2. \tag{6}$$

Introducing the following non-dimensional parameters:

$$x_1 = \frac{X_1}{a}, \quad x_2 = \frac{X_2}{b}, \quad \alpha = \frac{a}{b}, \quad \bar{w}(x_1, x_2, t) = w(x_1, x_2)\mathrm{e}^{\mathrm{i}\omega t} = W/a, \quad \mathrm{i} = \sqrt{-1}, \tag{7}$$

the above energy expressions can be written as

$$U = \frac{D_{11}}{2}\int_{-1/2}^{1/2}\int_{-1/2}^{1/2}\left[\frac{1}{\alpha}\left(\frac{\partial^2\bar{w}}{\partial x_1^2}\right)^2 + 2\nu_{21}\alpha\frac{\partial^2\bar{w}}{\partial x_1^2}\frac{\partial^2\bar{w}}{\partial x_2^2} + e\,\alpha^3\left(\frac{\partial^2\bar{w}}{\partial x_2^2}\right)^2 + 4\frac{D_{66}\alpha}{D_{11}}\left(\frac{\partial^2\bar{w}}{\partial x_1^2\partial x_2^2}\right)^2\right]\mathrm{d}x_1\,\mathrm{d}x_2, \tag{8a}$$

$$T = \frac{a^3 b}{2}\int_{-1/2}^{1/2}\int_{-1/2}^{1/2} \rho h\left(\frac{\partial\bar{w}}{\partial t}\right)^2 \mathrm{d}x_1\,\mathrm{d}x_2, \tag{8b}$$

$$F_s = \frac{a^2}{2}\sum_{i=1}^{4} k_i\bar{w}_i^2, \quad D = \frac{a^2}{2}\sum_{i=1}^{4} c_i(\dot{\bar{w}}_i)^2, \quad F_e = -aF(t)\bar{w}(0,0). \tag{8c-e}$$

In order to integrate the energy expressions in Eq. (8a–e), an area element with gridpoint designation shown in Fig. 2 is used. The derivative terms can be approximated in terms of discrete displacements at gridpoints by using the following finite difference operators:

$$\left(\frac{\partial^2\bar{w}}{\partial x_1^2}\right)_{m,n} = \frac{1}{\Delta x_1^2}(\bar{w}_{m-1,n} - 2\bar{w}_{m,n} + \bar{w}_{m+1,n}),$$

$$\left(\frac{\partial^2\bar{w}}{\partial x_2^2}\right)_{m,n} = \frac{1}{\Delta x_2^2}(\bar{w}_{m,n-1} - 2\bar{w}_{m,n} + \bar{w}_{m,n+1}), \tag{9}$$

$$\left(\frac{\partial^2\bar{w}}{\partial x_1\partial x_2}\right)_{m,n} = \frac{1}{4\Delta x_1\Delta x_2}(\bar{w}_{m-1,n-1} - \bar{w}_{m+1,n-1} - \bar{w}_{m-1,n+1} + \bar{w}_{m+1,n+1}),$$

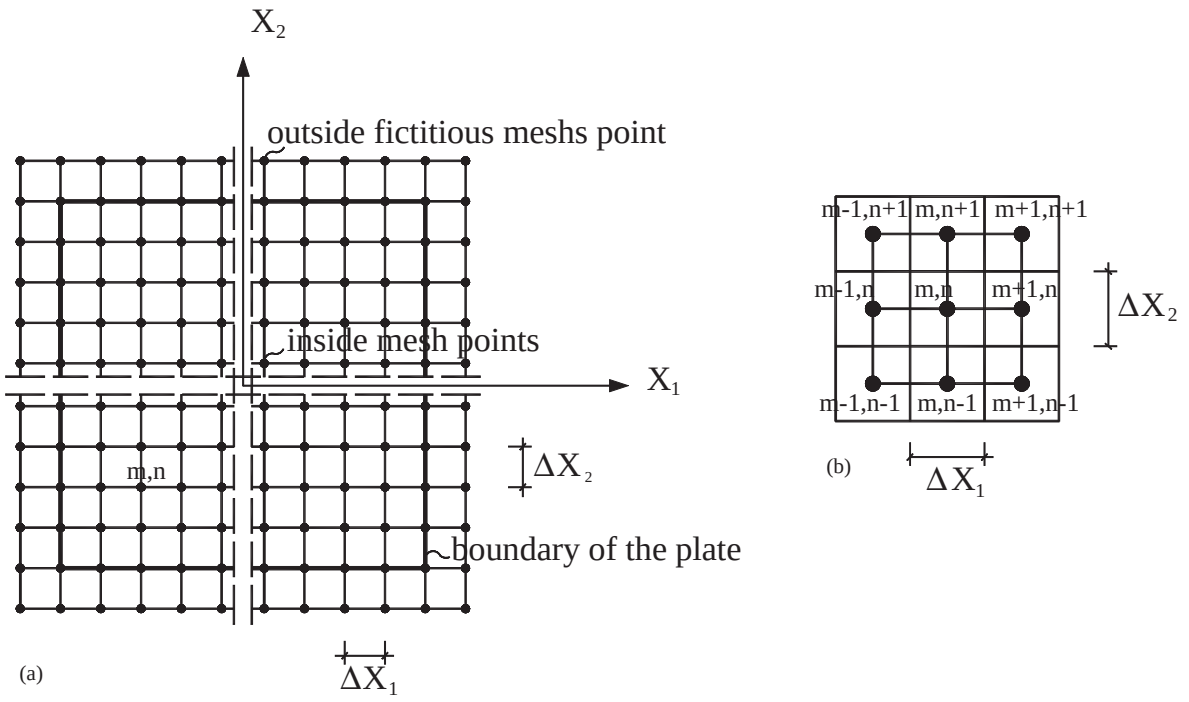

Fig. 2. (a) Fictitous and real mesh points of a full plate. Numbering of the mesh points when the pivotal point is m, n.

$$
\begin{aligned}
U_{m,n} = \frac{D_{11}}{2}\Bigg[& \frac{1}{\alpha\Delta x_1^4}(\bar{w}_{m-1,n} - 2\bar{w}_{m,n} + \bar{w}_{m+1,n})^2 \\
& + \frac{2\alpha\nu_{21}}{\Delta x_1^2\Delta x_2^2}(\bar{w}_{m-1,n} - 2\bar{w}_{m,n} + \bar{w}_{m+1,n})(\bar{w}_{m,n-1} - 2\bar{w}_{m,n} + \bar{w}_{m,n+1}) \\
& + \frac{4\alpha D_{66}}{D_{11}(4\Delta x_1^2\Delta x_2^2)^2}(\bar{w}_{m-1,n-1} - \bar{w}_{m+1,n-1} - \bar{w}_{m-1,n+1} + \bar{w}_{m+1,n+1}) \\
& + \frac{e\alpha^3}{\Delta x_2^4}(\bar{w}_{m,n-1} - 2\bar{w}_{m,n} + \bar{w}_{m,n+1})^2\Bigg]\alpha_{m,n}\Delta x_1\Delta x_2,
\end{aligned}
$$

$$
T_{m,n} = \frac{\rho h a^3 b}{2}\dot{\bar{w}}_{m,n}^2\Delta x_1\Delta x_2, \quad F_s = \frac{1}{2}a^2 k_s \bar{w}_{m,n}^2\alpha_s, \quad D = \frac{1}{2}a^2 c_s(\dot{\bar{w}}_{m,n})^2\alpha_s, \tag{10a–e}
$$

with

$$
\alpha_s = \begin{cases} 1 & \text{for pivotal point } m,\ n \text{ at the location of the support,} \\ 0 & \text{otherwise} \end{cases}
$$

and

$$
F_e = -aF(t)\bar{w}_{m,n}\alpha_Q
$$

where

$$\alpha_Q = \begin{cases} 1 & \text{for pivotal point } m,n \text{ at the plate center,} \\ 0 & \text{otherwise,} \end{cases}$$

in which $\alpha_{m,n}\Delta x_1\Delta x_1$ is the area element assigned to the location m,n in Fig. 2. The factor $\alpha_{m,n}$ is unity in the interior region of the plate, but it is $\frac{1}{2}$ when the pivotal point m,n is on the edge of the plate, and $\frac{1}{4}$ when it is at the corner of the plate.

The energy for the whole plate can be found by summing over the entire area of the plate. Thus

$$U = \sum_{m=1}^{N}\sum_{n=1}^{N} U_{m,n}, \quad T = \sum_{m=1}^{N}\sum_{n=1}^{N} T_{m,n}, \quad F_s = \sum_{i=1}^{4} F_{si},$$

$$D = \sum_{i=1}^{4} D_{ci}, \quad F_e = \sum_{i=1}^{1} F_{ei}, \tag{11}$$

where N is taken as the number of the mesh points in each of the two directions in the plate region as shown in Fig. 2a, $(N \times N)$ is the total number of the area elements on the plate. The governing differential equation as obtained from the Lagrange's equation is given as

$$\frac{\mathrm{d}}{\mathrm{d}t}\left(\frac{\partial T}{\partial \dot{\bar{w}}_{m,n}}\right) - \frac{\partial (T-U)}{\partial \bar{w}_{m,n}} + \frac{\partial D}{\partial \dot{\bar{w}}_{m,n}} + \frac{\partial F_s}{\partial \bar{w}_{m,n}} + \frac{\partial F_e}{\partial \bar{w}_{m,n}} = 0, \tag{12}$$

where $\bar{w}_{m,n}$ is the m, nth discrete displacement and the overdot stands for the partial derivative with respect to time. Introducing the following non-dimensional parameters,

$$\kappa_j = \frac{k_j a^3}{bD_{11}}, \quad \gamma_j = \frac{c_j}{\sqrt{\rho h D_{11}}}, \quad \lambda^2 = \frac{\rho h \omega^2 a^4}{D_{11}}, \quad q = \frac{Qa}{D_{11}} \tag{13}$$

and remembering that $\bar{w}(x_1, x_2, t) = w(x_1, x_2)\mathrm{e}^{\mathrm{i}\omega t}$, which was given in Eq. (7), by using Eq. (12) for the mesh point m, n with Eq. (10a–e) results in the following expression:

$$\begin{aligned}
&\left[-\frac{4}{\alpha\Delta x_1^4}(w_{m+1,n} - 2w_{m,n} + w_{m-1,n}) - \frac{4\nu_{21}\alpha}{\Delta x_1^2\Delta x_2^2}(w_{m,n-1} - 2w_{m,n} + w_{m,n+1})\right.\\
&\quad \left. - \frac{4\nu_{21}\alpha}{\Delta x_1^2\Delta x_2^2}(w_{m-1,n} - 2w_{m,n} + w_{m+1,n}) - \frac{4\alpha^3}{\Delta x_2^4}\frac{D_{22}}{D_{11}}(w_{m,n-1} - 2w_{m,n} + w_{m,n+1}) - \frac{2\lambda^2}{\alpha}w_{m,n}\right]\Delta x_{1(2)}\Delta x_{2(2)}\\
&\quad + \left[\frac{2}{\alpha\Delta x_1^4}(w_{m+2,n} - 2w_{m+1,n} + w_{m,n}) \frac{2\nu_{21}\alpha}{\Delta x_1^2\Delta x_2^2}(w_{m+1,n-1} - 2w_{m+1,n} + w_{m+1,n+1})\right]\Delta x_{1(3)}\Delta x_{2(2)}\\
&\quad + \left[\frac{2}{\alpha\Delta x_1^4}(w_{m,n} - 2w_{m-1,n} + w_{m-2,n}) + \frac{2\nu_{21}\alpha}{\Delta x_1^2\Delta x_2^2}(w_{m-1,n-1} - 2w_{m-1,n} + w_{m-1,n+1})\right]\Delta x_{1(1)}\Delta x_{2(2)}
\end{aligned}$$

$$+\left[\frac{2\nu_{21}\alpha}{\Delta x_1^2\Delta x_2^2}(w_{m+1,n-1}-2w_{m,n-1}+w_{m-1,n-1})+\frac{2\alpha^3}{\Delta x_2^4}\frac{D_{22}}{D_{11}}(w_{m,n-2}-2w_{m,n-1}+w_{m,n})\right.$$
$$\left.+\frac{2\nu_{21}\alpha}{\Delta x_1^2\Delta x_2^2}(w_{m+1,n-1}-2w_{m+1,n}+w_{m+1,n+1})\right]\Delta x_{1(2)}\Delta x_{2(1)}$$
$$+\left[\frac{2\nu_{21}\alpha}{\Delta x_1^2\Delta x_2^2}(w_{m+1,n+1}-2w_{m,n+1}+w_{m-1,n+1})+\frac{2\alpha^3}{\Delta x_2^4}\frac{D_{22}}{D_{11}}(w_{m,n}-2w_{m,n+1}+w_{m,n+2})\right]\Delta x_{1(2)}\Delta x_{2(3)}$$
$$+\left[\frac{\alpha}{\Delta x_1^2\Delta x_2^2}\frac{D_{66}}{2D_{11}}(w_{m-2,n-2}-w_{m-2,n}-w_{m,n-2}+w_{m,n})\right]\Delta x_{1(1)}\Delta x_{2(1)}$$
$$+\left[-\frac{\alpha}{\Delta x_1^2\Delta x_2^2}\frac{D_{66}}{2D_{11}}(w_{m-2,n}-w_{m-2,n+2}-w_{m,n}+w_{m,n+2})\right]\Delta x_{1(1)}\Delta x_{2(3)}$$
$$+\left[-\frac{\alpha}{\Delta x_1^2\Delta x_2^2}\frac{D_{66}}{2D_{11}}(w_{m,n-2}-w_{m,n}-w_{m+2,n-2}+w_{m+2,n})\right]\Delta x_{1(3)}\Delta x_{2(1)}$$
$$+\left[\frac{\alpha}{\Delta x_1^2\Delta x_2^2}\frac{D_{66}}{2D_{11}}(w_{m,n}-w_{m,n+2}-w_{m+2,n}+w_{m+2,n+2})\right]\Delta x_{1(3)}\Delta x_{2(3)}$$
$$+\frac{2(\kappa+\mathrm{i}\lambda\gamma)}{\Delta x_1\Delta x_2}w_{m,n}\alpha_s=\frac{\alpha_Q\, q}{\Delta x_1\Delta x_2},\quad \mathrm{i}=\sqrt{-1}. \tag{14}$$

For the whole mesh points, by using Eq. (14), the following set of linear algebraic equations is obtained which can be expressed in the following matrix form:

$$[\mathbf{A}]\{\mathbf{w}\}+\mathrm{i}\lambda\gamma[\mathbf{B}]\{\mathbf{w}\}-\lambda^2[\mathbf{C}]\{\mathbf{w}\}=\{\mathbf{q}\}, \tag{15}$$

where [**A**], [**B**] and [**C**] are coefficient matrices obtained by using Eq. (14) for all mesh points.

For free vibration analysis, when the external force and damping of the supports are zero in Eq. (15), this situation results in a set of linear homogeneous equations that can be expressed in the following matrix form:

$$[\mathbf{A}]\{\mathbf{w}\}-\lambda^2[\mathbf{C}]\{\mathbf{w}\}=\{\mathbf{0}\}. \tag{16}$$

Numbering of the mesh points is shown in Fig. 2b. By decreasing the dimensionless mesh widths, $\Delta=\Delta x_1=\Delta x_2$, the accuracy can be increased.

The total magnitude of the reaction forces of the supports is given by

$$\sum_{j-1}^{4}P_i=\sum_{j-1}^{4}(k_j+\mathrm{i}c_j w)aw(x_{1j},x_{2j}), \tag{17}$$

and therefore the force transmissibility at the supports is determined by

$$T_R=\sum_{j-1}^{4}P_i/F=\sum_{j-1}^{4}(\kappa_j+\mathrm{i}\gamma_j\lambda)w(x_{1j},x_{2j})/q. \tag{18}$$

The number of unknown displacements is $(N+2)^2$, where N^2 is the mesh size in the plate region. Again, the number of equations which can be written for each point in the plate region and outside the plate region by using Eq. (14) is $(N+2)^2$, which is given in matrix form by Eq. (15).

Therefore, the total number of these equations is equivalent to the total number of unknown displacements and these unknowns can be determined by using the above mentioned equations.

3. Numerical results

The steady state response to a point force $F(t)$ acting at the center of an orthotropic square plate, viscoelastically supported at four points which are symmetrically located at the corners or on the two diagonals, is calculated numerically. The parameters κ_i and γ_i are taken as having the same respective values at all the supports denoted by $\kappa_i = \kappa_s$ and $\gamma_i = \gamma_s$. Because of the structural symmetry and symmetry of the external force, only symmetrical vibrations arise in the plate. The symbol SS represents symmetrical vibration with respect to centerlines.

A short investigation of the free vibration of an elastically point-supported plate is necessary for comparing the obtained results with the existing results and for a better understanding of the responses presented in this study. The natural frequencies of the elastically point-supported plate are determined by calculating the eigenvalues λ of the frequency equation obtained by taking the damping parameter of the supports as $\gamma_s = 0$ and $q = 0$ in Eq. (15). In the case $\gamma_s = 0$ and $q = 0$, the obtained results for $\kappa = 0$ and $\kappa = \infty$ correspond to those of completely free and point-supported plates respectively. These results are tabulated and compared with the existing results for completely free and point-supported plates in Table 1. Also, the mode shapes of the vibration can be determined from Eq. (16) by taking a displacement as known and calculating the eigenvectors corresponding to the eigenvalues. In Table 2, the frequencies at which the peak values of the force transmissibilities occur are determined for various damping parameters γ_s for $\kappa_s = 100$ by using Eqs. (15) and (18). As far as the authors know, there are no results to compare the results given in Table 2. It should be noted that in Fig. 3a, the comparison of the variation of the frequency parameter with κ_s is for $E_2/E_1 = 1$, $E_2/E_1 = 0.8$, $E_2/E_1 = 0.6$ and the mesh size is (31×31) in the case $\gamma_s = 0$. In all of the numerical calculations, ν_{21} is taken as 0.3 and the locations of the point supports are chosen at the corners of the plate. In Fig. 3a, the values of the ordinates at $\kappa_s = 0$ and $\kappa_s = \infty$, respectively, represent the frequency parameters of an unconstrained free plate and a simply point-supported plate. When increasing the parameter κ_s, the frequency parameters increase monotonically and ultimately become the values of a simply point-supported plate. In the isotropic case, nodal lines arising in the $SS-2$ vibration mode coincide with the diagonals passing through the supports for $E_2/E_1 = 1$ as seen in the mode shapes, Fig. 3b, and therefore the frequency parameter remains constant without being affected by the variation of κ_s [1,2], as can be seen from Fig. 3a. However, in the orthotropic case, nodal lines arising in the $SS-2$ vibration mode do not coincide with diagonals, (Fig. 3b, $SS-2$ mode) and their shapes change with the variation in κ_s [1]. In the $SS-3$ mode, the circle changes its shape when the plate is orthotropic; but this difference is very small for the parameters considered.

In Fig. 4a–c, the convergence of the $SS-1$, $SS-2$ and $SS-3$ modes are presented, respectively, for the following orthotropy values: $E_2/E_1 = 1$, $E_2/E_1 = 0.8$, $E_2/E_1 = 0.6$. It is shown that the convergence with respect to mesh size is quite good in the considered cases. As it is observed from Fig. 4a–c, the frequency parameter increases as the mesh size increases: It means that the convergence is from below for the considered symmetric modes, and with increasing the mesh size the exact value can be approached from below. But, the convergence can be from above

Table 1
Frequency parameters λ for a free and simply point-supported orthotropic square plate supported at the corners: $v_{21} = 0.3$, $\gamma_s = 0$

Vibration mode	E_2/E_1	Kocatürk		Present		Narita [5] point sup.	Venkateswara et al. [6] point sup.
		$\kappa_s = 0$	$\kappa_s = \infty$	$\kappa_s = 0$	$\kappa_s = \infty$		
$SS-1$	1.0	0	7.139	0	7.107	7.1189	7.11088
	0.8	0	6.815	0	6.686		
	0.6	0	6.326	0	6.083		
$SS-2$	1.0	19.684	19.684	19.579	19.579	19.5961	19.5961
	0.8	18.033	18.329	17.877	18.212		
	0.6	15.674	16.839	15.496	16.643		
$SS-3$	1.0	24.347	44.383	24.248	44.292	44.3696	—
	0.8	23.508	43.237	23.339	41.642		
	0.6	22.981	41.786	22.757	38.447		

Table 2
The frequencies at which the peak values of the force transmissibilities occur: $v_{21} = 0.3$

	e	$\gamma_s = 0$	$\gamma_s = 1$	$\gamma_s = 5$	$\gamma_s = 10$	$\gamma_s = 25$	$\gamma_s = 50$	$\gamma_s = 100$	$\gamma_s = 500$	$\gamma_s = 1000$
$SS-1$	1.0	6.722	6.723	6.754	6.829	7.003	7.076	7.088	7.107	7.107
	0.8	6.361	6.362	6.387	6.448	6.591	6.657	6.679	6.686	6.686
	0.6	5.837	5.838	5.853	5.893	6.002	6.057	6.076	6.083	6.083
$SS-2$	0.8	18.192	18.192	18.186	18.320	18.214	18.212	18.212	18.212	18.212
	0.6	16.572	16.571	16.548	16.948	16.653	16.649	16.644	16.643	16.643
	1.0	40.603	40.993	43.559	44.089	44.259	44.285	44.290	44.292	44.292
$SS-3$	0.8	38.591	38.912	40.985	41.453	41.611	41.638	41.641	41.642	41.642
	0.6	36.212	36.433	37.922	38.295	38.427	38.441	38.446	38.447	38.447

or below for the present solution method. The reason of this situation can be understood by the following remark given by Johns and Nagaraj [4]: 'It should be remembered that energy methods always overestimate the fundamental frequency, so with more refined analyses the exact value can be approached from above. Conversely, the finite difference method appears to underestimate the natural frequency and with increasing refinement in the analysis the exact value can be approached from below'. However, in the present study, by introducing the constant $\alpha_{m,n}$ the energy is estimated realistically and therefore the convergence characteristic of the finite difference technique becomes dominant, namely the convergence is from below in the present study for the considered modes. Also, it should be noted that, the results for the in-between mesh sizes always fall between those of the upper and lower mesh sizes. In Table 1, the obtained results are compared with those of obtained by Kocatürk [1] for a completely free and a corner point-supported orthotropic square plate. It is observed from Table 1 that the results are in good

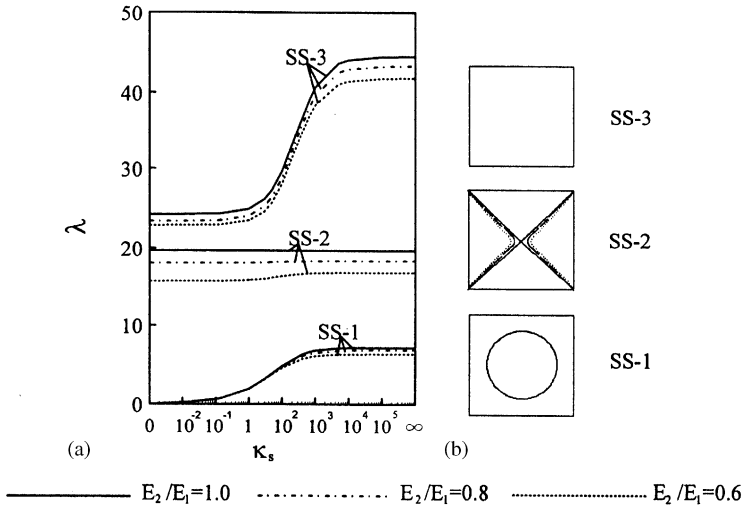

Fig. 3. (a) Frequency parameters of square orthotropic plates elastically supported at the corners. $v_{21} = 0.3$. (b) Frequency parameters of square orthotropic plates elastically supported at four points symmetrically located on the diagonals. $v_{21} = 0.3$; $\kappa_s = 100$. The nodal patterns for the $SS-1$, $SS-2$ and $SS-3$ vibrations.

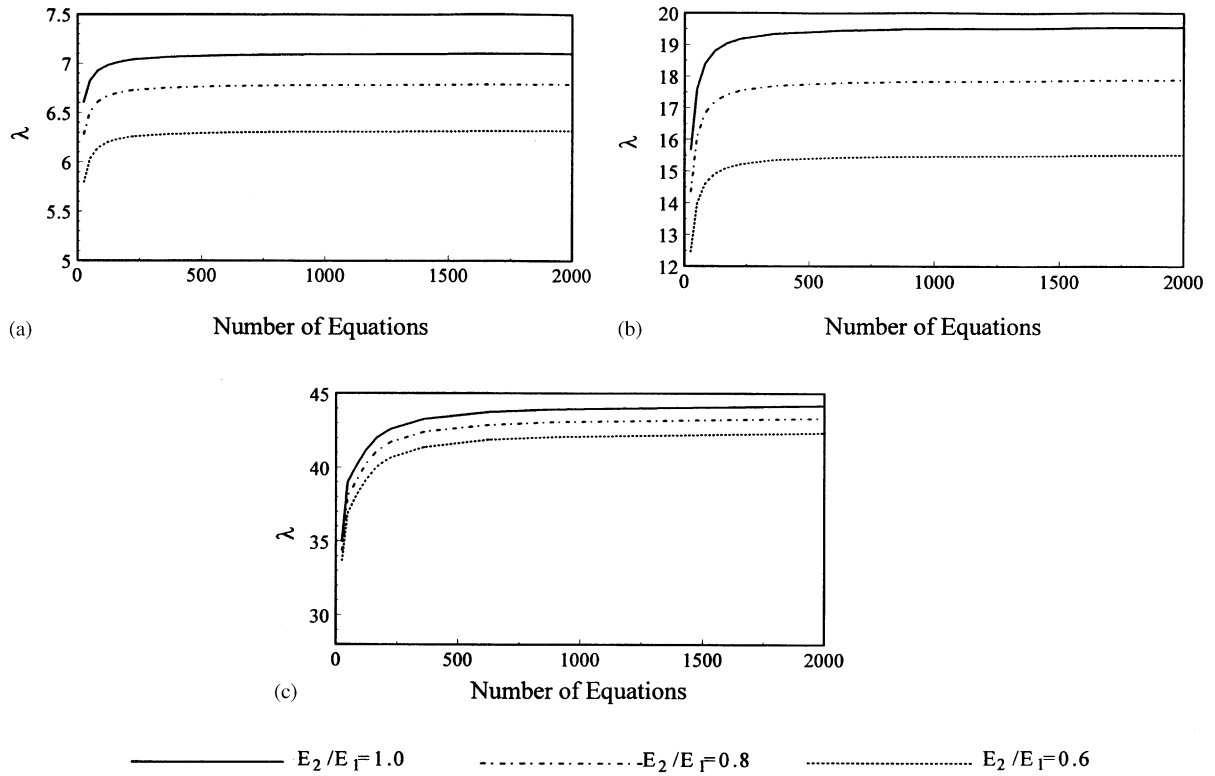

Fig. 4. (a) Convergence of the $SS-1$ mode. $\kappa_s = \infty$. (b) Convergence of the $SS-2$ mode. $\kappa_s = \infty$. Convergence of the $SS-3$ mode. $\kappa_s = \infty$.

agreement. Also the results for the corner point supports obtained by Narita [5] by using the classical Ritz method and by Venkateswara Rao et al. [6] by using a finite element method for the first three SS modes are given again in Table 1, and are in better agreement with the present results than those of Kocatürk [1] and Yamada et al. [2]. Fig. 5 shows the force transmissibilities for various E_2/E_1 values for a viscoelastically point-supported plate for $\gamma_s = 1$, $\kappa_s = 100$. It is observed from Fig. 5 that, when E_2/E_1 ratio is different from unity, the $SS-2$ mode occurs. This result was also determined by Kocatürk [1].

Fig. 6 and also Fig. 5 show that within the frequency range of the figures, when E_2/E_1 ratio is different from unity, three resonant peaks appear for the $SS-1$, $SS-2$ and $SS-3$ vibrations, and also antiresonant peaks or lowest values appear between adjacent frequencies. In Fig. 6, the solid lines ($\gamma_s = 0$) represent the response curve of a plate with undamped elastic point support, and the dotted lines ($\gamma_s = \infty$) a plate with simple supports. The four points of intersection p, r, s, t of these two lines are fixed points, through which all the response curves pass, regardless of the damping parameters. This result was also determined by Yamada et al. [2] for isotropic viscoelastically point-supported plates. By choosing a suitable value for the damping parameter γ_s, it is possible to reduce the peak values of the force transmissibilities to the values of the force transmissibilities which correspond to the points p, r, s, t, Fig. 6a–c. To show this situation better, the considered frequency regions are expanded and shown on the right-hand sides of Fig. 6a for the $SS-1$ mode, Fig. 6b and c for the $SS-2$ mode. Existence of such points is useful for an optimum design of a system by choosing appropriate damping parameter. Within a certain range of the frequencies, the force transmissibilities are less than unity, which indicates the possibility of vibration isolation. When E_2/E_1 is unity, the $SS-2$ vibration with nodal lines passing through the supports does not arise in the plate. Therefore, in the case of $SS-2$ mode, the peak values of the force transmissibilities do not occur for the isotropic case and the line for this mode in Table 2 is not shown.

Fig. 7 shows that with the variation of damping parameter γ_s, there is a damping parameter for which the values of the resonant peaks are minimum. The resonant peaks occur at different values of λ while changing the damping parameter γ_s. However, the frequency parameter λ remains between the frequency parameters λ obtained for $\gamma_s = 0$ and ∞. Therefore, in Fig. 7, while changing γ_s for obtaining minimum peak value of the force transmissibility for the considered mode, the frequency parameter λ also changes a little. As it was explained before, λ changes between λ obtained for $\gamma_s = 0$ and λ obtained for $\gamma_s = \infty$. From Fig. 7, it is concluded that there is

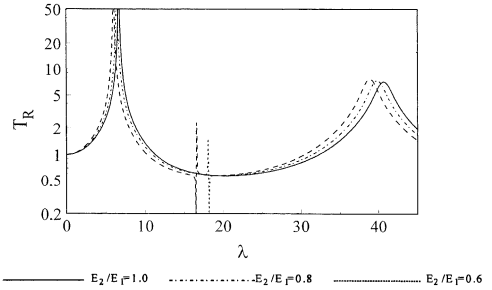

Fig. 5. The force transmisibilities of square orthotropic plates for various E_2/E_1 values for corner supported plate. $\gamma_s = 1$; $\nu_{21} = 0.3$; $\kappa_s = 100$.

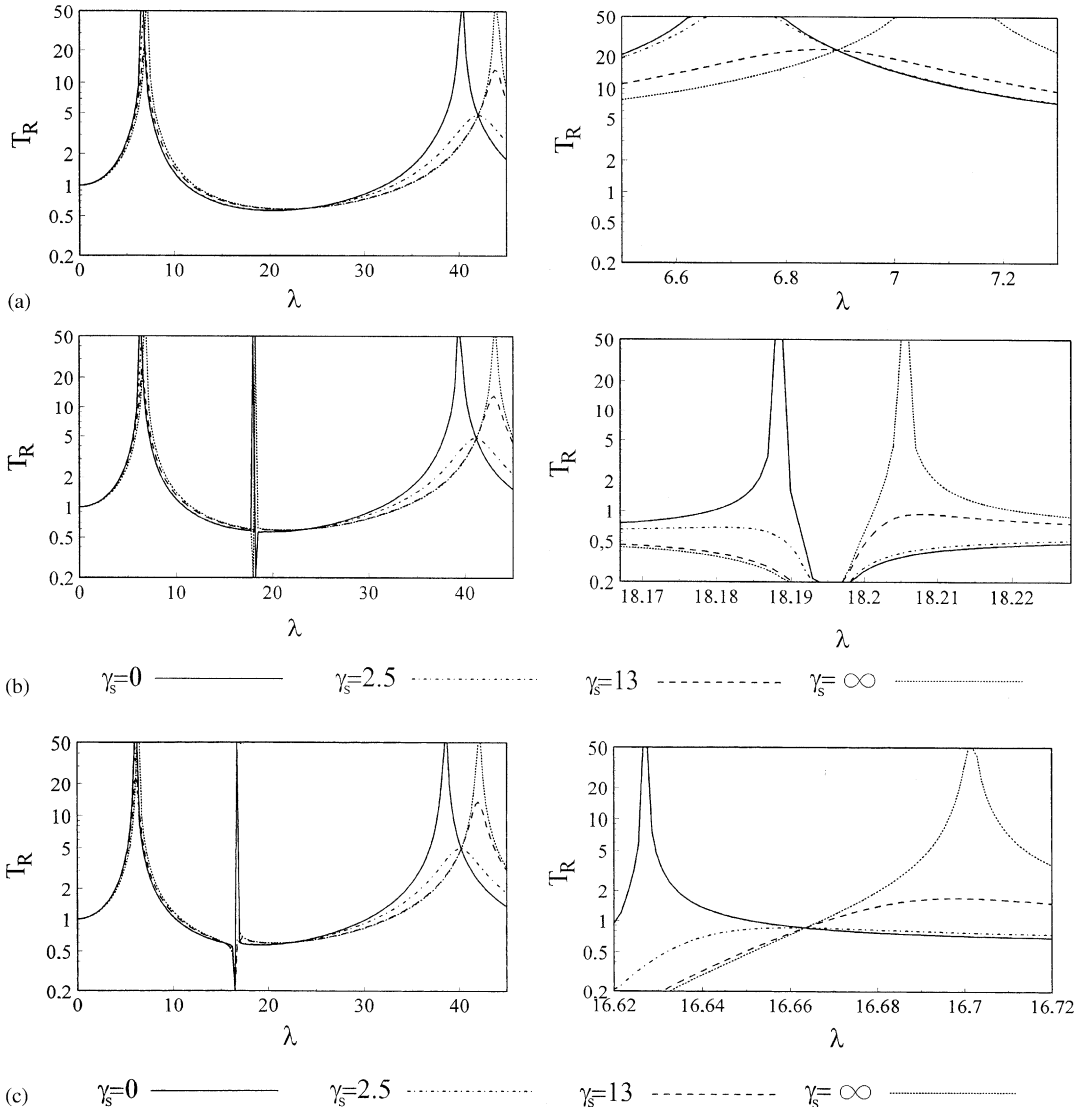

Fig. 6. The force transmissibilities of square orthotropic plates viscoelastically supported at the corners under the action of the center-force for various γ_s values for (a) $E_2/E_1 = 1.0$; (b) $E_2/E_1 = 0.8$; and (c) $E_2/E_1 = 0.6$. $v_{21} = 0.3$; $\kappa_s = 100$.

a certain value of γ_s at which the resonant peaks become minimum. Figs. 6a and 7a show that, for $\gamma_s = 13$, at $\lambda = 6.9$, the minimum peak value of the force transmissibility is 22.9 for the $SS-1$ mode for $E_2/E_1 = 1$. It is observed from Figs. 6a and 7c that for $\gamma_s = 2.5$, at $\lambda = 42.03$, the minimum peak value for the third mode is 5.0 for $E_2/E_1 = 1$. It is seen from Figs. 6c and 7b that, for $\gamma_s = 2.7$, at $\lambda = 16.662$, the minimum peak value of the force transmissibility is 0.8 for the $SS-2$ mode for $E_2/E_1 = 0.6$. Because the damping parameters for the minimum peak values of the force transmissibilities for the $SS-1$ and $SS-2$ modes for $E_2/E_1 = 1$, $E_2/E_1 = 0.8$,

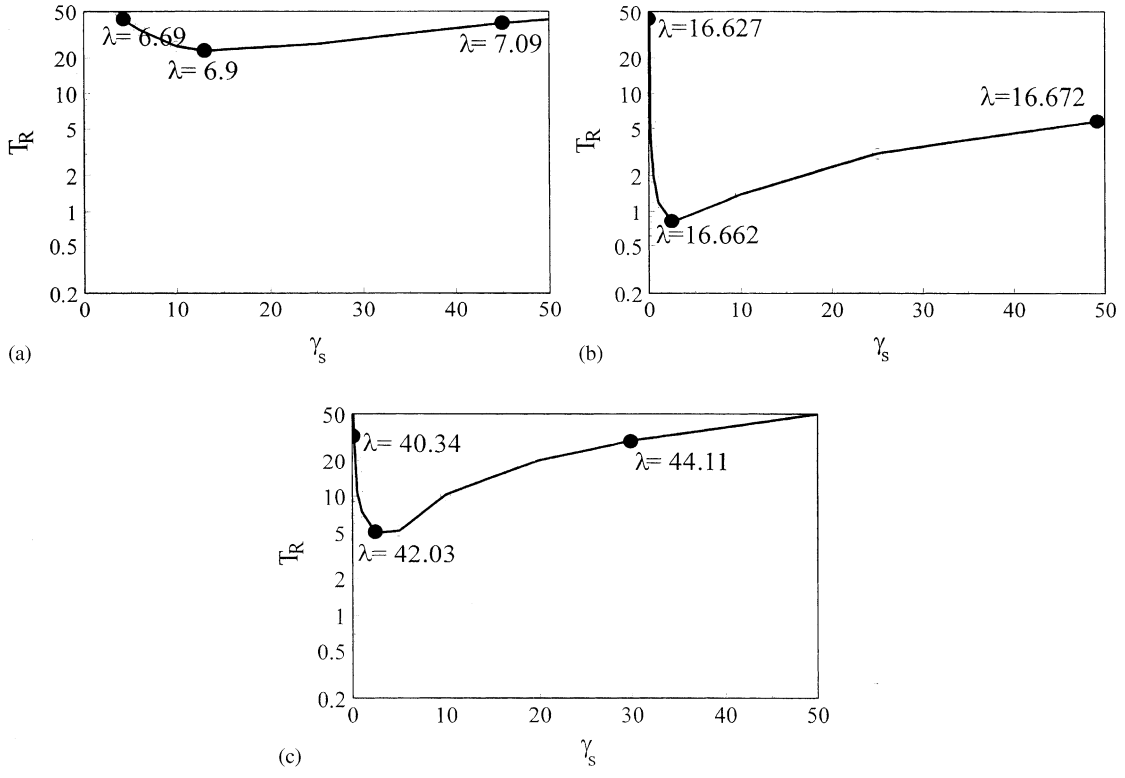

Fig. 7. The minimum resonant peak values with the variation of γ_s for (a) $SS-1$ mode, $E_2/E_1 = 1.0$; (b) $SS-2$ mode, $E_2/E_1 = 0.6$; and (c) $SS-3$ mode, $E_2/E_1 = 1.0$. $\nu_{21} = 0.3$; $\kappa_s = 100$.

$E_2/E_1 = 0.6$ orthotrophy ratios are very close to each other, the minimum peak values of the force transmissibilities with the variation of damping parameter γ_s for $E_2/E_1 = 0.8$, $E_2/E_1 = 0.6$ are not shown in the figures.

4. Conclusions

By using an energy-based finite difference method, the steady state response of a viscoelastically point-supported orthotropic square plate to a sinusoidally varying force has been studied and compared with the existing results.

By the application of the above-mentioned solution technique, the first three SS natural frequencies are determined, the converge characteristics of the frequency parameters are investigated and the response curves to a sinusoidally varying point force acting at the center are determined numerically for orthotropic square plates viscoelastically supported at four points at the corners. The effect of the orthotropy on the frequency parameters and response curves is investigated. It is seen that, because of the orthotropy, the $SS-2$ mode occurs in the plate and this mode may be more important than the others for some orthotrophy ratios. Also, the frequency ranges, where the vibration isolation occurs, are determined and the damping ratio

values for obtaining minimum peak values of force transmissibilities are obtained for some considered parameters. These obtained results may easily be extended to multiple support conditions and may be useful for designing mechanical and structural systems under external dynamic loads. The solution procedure followed here can easily be used for various support and loading conditions.

References

[1] T. Kocatürk, Determination of the steady state response of viscoelastically point-supported rectangular anisotropic (orthotropic) plates, Journal of Sound and Vibration 213 (1998) 665–672.
[2] G. Yamada, T. Irie, M. Takahashi, Determination of the steady state response of viscoelastically point-supported rectangular plates, Journal of Sound Vibration 102 (1985) 285–295.
[3] J.P. Singh, S.S. Dey, Parametric instability of rectangular plates by the energy based finite difference method, Computer Methods in Applied Mechanics and Engineering 97 (1992) 1–21.
[4] D.J. Johns, V.T. Nagaraj, On the fundamental frequency of a square plate symmetrically supported at four points, Journal of Sound and Vibration 10 (1969) 404–410.
[5] Y. Narita, Note on vibrations of point supported rectangular plates, Journal of Sound and Vibration 93 (1984) 593–597.
[6] G. Venkateswara Rao, I.S. Raju, C.L. Amba-Rao, Vibrations of point supported plates, Journal of Sound and Vibration 29 (1973) 387–391.